Title

Estimating Optical Coherence Tomography Structural Measurement Floors to Improve Detection of Progression in Advanced Glaucoma

Authors

Bowd, Christopher
Zangwill, Linda M
Weinreb, Robert N
et al.

Publication Date

2017-03-01

DOI

10.1016/j.ajo.2016.11.010

Peer reviewed

HHS Public Access

Author manuscript

Am J Ophthalmol. Author manuscript; available in PMC 2018 March 01.

Published in final edited form as:

Am J Ophthalmol. 2017 March ; 175: 37–44. doi:10.1016/j.ajo.2016.11.010.

Estimating OCT Structural Measurement Floors to Improve Detection of Progression In Advanced Glaucoma

Christopher Bowd, **Linda M. Zangwill**, **Robert N. Weinreb**, **Felipe A. Medeiros**, and **Akram Belghith**

Hamilton Glaucoma Center, Department of Ophthalmology and Shiley Eye Institute, University of California, San Diego, La Jolla, CA 92093-0946

Abstract

Purpose—"Floor effects" in retinal imaging are defined as the points at which no further structural loss can be detected. We estimated the measurement floors for spectral-domain optical coherence tomography (SD-OCT) measurements and compared global change over time in advanced glaucoma eyes.

Design—Validity study to investigate measurement floors.

Methods—A longitudinal "Variability Group" of 41 eyes with moderate to advanced glaucoma (SAP MD ≤ −8 dB) was used to estimate measurement floors. Minimum rim width (MRW), ganglion cell-inner plexiform layer thickness (GC-IPLT) and circumpapillary retinal nerve fiber layer thickness (cpRNFLT) were determined. Floors were defined as the average image area with a loss < 1st percentile confidence interval of the variability in this group. Global rate of change and percentage of the region of interest that did not reach the measurement floor at baseline were calculated in 87 eyes with advanced glaucoma (SAP MD ≤ −12 dB).

Results—Global change over time in longitudinal eyes was −1.51 μm/year for MRW, −0.21 μm/year for GC-IPL and −0.36 μm/year cpRNFL (all p≤0.03). The percentage of region of interest that did not reach the floor at baseline was 19% for MRW, 36% for GC-IPLT and 14% for cpRNFLT. Average (±S.D.) floors were 105 μm (±15.9 μm) for MRW, 38 μm (±3.4 μm) for GC-IPLT and 38 μm (±4.2 μm) for cpRNFLT.

Corresponding Author: Akram Belghith, Ph.D., Hamilton Glaucoma Center, Department of Ophthalmology, University of California, San Diego, La Jolla, CA, 92037-0946, abelghith@ucsd.edu.

Financial Disclosures:
Bowd: (No financial disclosure)
Zangwill: (Financial support in the form of research instrument provision: Carl Zeiss Meditec Inc., Heidelberg Engineering GmbH, Optovue Inc., Topcon Medical Systems Inc.)
Weinreb: (Financial support in the form of research instrument provision: Carl Zeiss Meditec Inc., Heidelberg Engineering GmbH, Optovue Inc., Topcon Medical Systems Inc.; Consultant: Alcon Laboratories Inc., Allergan Inc., Bausch and Lomb).
Medeiros: (Financial support in the form of research funding: Carl Zeiss Meditec Inc., Heidelberg Engineering GmbH, Topcon Medical Systems Inc.; Consultant: Alcon Laboratories Inc., Allergan Inc., Reichert Technologies).
Belghith: (None).
Other: None.

Conclusions—In advanced glaucoma, more GC-IPL tissue remains above the measurement floor compared to other measurements, suggesting GC-IPL thickness is the better candidate for detecting progression. Progression in SD-OCT measurements is observable in advanced disease.

Glaucoma is a progressive optic neuropathy that can result in irreversible loss of visual function in response underlying structural changes.[1,2] Detecting worsening of the disease is an essential part of glaucoma management, as health care providers worldwide must determine whether the patient is stable and current treatment is effective or if the patient is progressing and treatment must be modified.

Optical imaging using spectral domain optical coherence tomography (SD-OCT) currently is the standard of care for the early detection and monitoring of glaucoma based on anatomical abnormality [e.g., retinal nerve fiber layer (RNFL) thinning and more recently macular thinning[3–6]]. Some evidence exists, however, that in advanced disease, SD-OCT measurements are not useful for measuring tissue thickness because of the presence of a floor effect, after which no more thinning is observable.[7–11] This floor effect, possibly due to the presence of residual tissue (e.g., glial cells, blood vessels[12]) or failure of tissue segmentation algorithms (i.e., an artifactual floor)[13], is thought to be a serious problem for monitoring structural changes in eyes with advanced glaucoma. Even though the patient with advanced disease may be progressing, it is often challenging to detect any observable change with optical imaging. In these eyes, monitoring of disease must rely on standard automated perimetry (SAP) or other visual function tests. Although SAP is a standard clinical test, SAP measurements of visual sensitivity are notoriously variable, particularly as glaucoma severity increases.[14–16]

Ideally, some SD-OCT measured anatomical structures would reach a measurement floor further along the disease continuum than others. If this were the case, certain structures would prove more valuable for assessing structural progression in advanced glaucoma than others. The purposes of the current study were 1) to estimate the measurement floors of several SDOCT- measured retinal structures: minimum rim width (MRW), ganglion cell-inner plexiform layer (GC-IPL) thickness and circumpapillary RNFL (cpRNFL) thickness; from raw 3D images in eyes with advanced but stable glaucoma, 2) to report the percentage of the whole image area of eyes that had not reached the measurement floor in an independent test sample of baseline measurements from advanced glaucoma eyes and 3) to determine if significant change over time of these measurements is observable in advanced glaucoma eyes. The results should be relevant to the SD-OCT measurements most suitable for detecting change in eyes with advanced disease.

METHODS

128 eyes from 86 glaucoma patients enrolled in the UC San Diego Diagnostic Innovations in Glaucoma Study (DIGS) were included in the current analysis. The DIGS is a prospective longitudinal study designed to evaluate optic nerve structure and visual function in glaucoma that follows the same protocol as the UC San Diego-based African Descent and Glaucoma Evaluation Study.[17] Enrollment of participants is based on the inclusion/exclusion criteria specified below. The UC San Diego Human Research Protection Program/Institutional

Review Board approved all methodology and all methods adhered to the tenets of the Declaration of Helsinki for research involving human subjects and to the Health Insurance Portability and Accountability Act. The DIGS was registered at http://cilincaltrials.gov (NCT00221897) on September 14, 2005.

Eligible participants had best corrected visual acuity of 20/40 or better, spherical refraction within ±5.0 Diopter (D), cylinder correction within ±3.0 D, and open angles on gonioscopy. All participants were older than 18 years. Participants were excluded if they had a history of intraocular surgery (except for uncomplicated cataract or glaucoma surgery). Eyes with coexisting retinal disease, uveitis or non-glaucomatous optic neuropathy were excluded from the investigation. Diabetic participants with no evidence of retinal involvement were included. Self-reported information regarding systemic conditions, medications and risk factors associated with glaucoma was recorded. For glaucoma subjects, inclusion criteria were: 1) open angles on gonioscopy and 2) at least 2 consecutive standard automated perimetry visual field (VF) examinations with either a pattern standard deviation (PSD) ≤ 0.5 or a glaucoma hemifield test (GHT) result outside the 99% normal limits.

Participants and Testing

All subjects underwent an annual comprehensive ophthalmologic examination including review of medical history, best-corrected visual acuity, slit-lamp biomicroscopy, dilated funduscopic examination, and stereoscopic optic disc photography. Semi-annual examination included intraocular pressure (IOP), SD-OCT imaging and VF testing.

Two independent groups of glaucoma eyes, as defined above, were assessed for the analyses. All VF results were reliable with fixation losses ≤ 33%, false positive responses ≤ 15% with no apparent test artifacts as assessed by technicians for the UC San Diego Visual Field Assessment Center (VisFACt).

A Variability Group of 41 eyes of 27 glaucoma patients with moderate to advanced glaucoma (mean deviation; MD ≤ −8 dB) with repeated tests over 5 weeks was used to estimate the measurement floors (The Variability Group is named as such because testing was frequent over a time frame that should not show progressing glaucomatous change, rather just measurement variability). Eighty-seven eyes of 59 patients with advanced to severe glaucoma (SAP MD ≤ −12 dB[18]) imaged twice over the course of approximately two years were included in a Longitudinal Group.

All eyes underwent two 24-2 SAP exams prior to baseline imaging to be classified as glaucomatous and were imaged using Spectralis© SD-OCT (software version 5.2.0.3, Heidelberg Engineering GmbH) two or more times. Scan protocols used were the enhanced depth imaging (EDI) optic nerve head-centered radial scan (48 B-scans * 768 A-scans each), the high-resolution macular cube scan (73 B-scans * 768 A-scans each) and the high-resolution optic disc cube scan (73 B-scans * 768 A-scans each). Overall quality of OCT scans was evaluated by UC San Diego Imaging Data Evaluation and Assessment (IDEA) Center technicians and all scans were considered of acceptable quality based on standardized assessment protocol.

A summary of the demographic variables and measurements at baseline for each group are shown in Table 1. Glaucoma patients in the Longitudinal Group were significantly older ($p < 0.001$) and had worse visual field MD ($p < 0.001$) than those in the Variability Group (the latter difference by design). Participants in the Longitudinal and Variability groups were similar with respect to gender ($p = 0.68$), axial length ($p = 0.44$) and optic disc area ($p = 0.41$).

Retinal Layer Segmentation

Raw SD-OCT thickness maps were exported to a numerical computing language (MATLAB, The MathWorks, Natick, MA). The MRW, GC-IPL and cpRNFL layer thicknesses were segmented from the raw images (from the three scan protocols described above) using the San Diego Automated Layer Segmentation Algorithm (SALSA). SALSA has been described previously[19–21] and was used to automatically segment 1) the Bruch's membrane opening (BMO) and the internal limiting membrane (ILM) on each ONH radial B-scan to calculate the MRW defined as the shortest distance from BMO to ILM, 2) the macular GC-IPL thickness from the macular cube scan and 3) the cpRNFL thickness from the optic disc cube scan.

SALSA is based on the assumption that each B-scan consists of several inter-retinal layers [e.g., the Bruch's membrane (BM) layer, the cpRNFL]. Briefly, each retinal layer was defined by a curve modeling its skeleton and a filter, or set of filters, modeling its thickness. In this study, we were only interested in the segmentation of the BM and ILM layers in the ONH radial scans and the GC-IPL and cpRNFL layers in the macular and ONH cube scans. An object-oriented approach where segments of the layer are generated was utilized to build connected skeletons rather than a voxel-oriented approach. A Monte Carlo Markov Chain approach was used estimate the model parameters and hyper-parameters.[22]

Defining the Measurement Floors

For each structural measurement, we defined local variability to assess change over time in the Longitudinal Group. Specifically, for MRW, local variability was calculated at 96 MRW locations defined by each of the 48 radial B-scans (intersecting at each side of the BMO). For GC-IPL and cpRNFL thickness maps, local variability was calculated from a 5,906 superpixel grid (sized 2 pixels * 5 pixels) comprising the total 73 B-scan * 768 A-scan (56,065 pixels) macular cube image and optic disc cube image, respectively. Theoretically for cpRNFL images, because the size of the optic disc varies by eye, the number of available super-pixels used to define the image area also varies by eye. To control for this potential confounder, optic disc area was standardized on all images to be equal to the 95% confidence interval (CI) of optic disc area of all eyes included in the study, 2.91 mm^2. To reduce the variability of fovea-to-disc angle across eyes, we normalized the fovea-to-disc angle to −6 deg for all eyes.[23]

To define the measurement floors we plotted the distribution of the variability of the slopes of linear regression of MRW, GC-IPL thickness and cpRNFL thickness at each location (from MRW locations and GC-IPL and cpRNFL grids, described above) over 5 imaging sessions obtained from eyes composing the Variability Group. The floor for each structural

measurement was defined based on the image area with a loss less than the 1st percentile confidence interval of the variability observed in this group. This cut-off was selected to minimize the false positive rate (i.e., to minimize the chance of potential glaucoma progression diagnostic regions being assigned as floor regions). The average percentage of image area useable to assess glaucoma progression over time in advanced glaucoma eyes also was calculated.

ANALYSES

Demographic characteristics by group (Variability versus Longitudinal) were compared using descriptive statistics. Categorical variables were compared using Chi^2 tests and continuous variables were compared using t-tests (Table 1).

Ordinary least square linear regression was used to calculate the structural loss from baseline (i.e., the slope) for each area of MRW, macular GC-IPL thickness map and cpRNFL thickness map. Multivariable models included Group (Variability Group vs. Longitudinal Group), Time and the interaction term Group * Time. P-values less than 0.05 were considered statistically significant. Statistical analyses were performed using SAS, Version 9.2 (SAS Institute, Cary, NC, USA).

For each structural measurement, the Variability group was used to determine the variability at each radial scan for MRW and for each superpixel for GC-IPL and cpRNFL thickness. Therefore any change beyond this variability in the glaucoma group was due to either rapid disease related change or age related change (the latter is less likely with two years follow-up and on two visits).

RESULTS

Baseline global MRW derived from the ONH radial scan, macular GC-IPL thickness derived from the macular cube scan and cpRNFL thickness derived from the ONH cube scan measurements in eyes from the Variability Group and the Longitudinal Group are presented in Table 2. Eyes from the Variability Group had thicker baseline MRW, GC-IPL thickness and cpRNFL thickness than eyes from the Longitudinal Group (all $p < 0.001$), likely a result of the selected difference in SAP severity between groups.

Average structural loss across the whole thickness map over time of MRW, macular GC-IPL thickness and cpRNFL thickness in the Variability Group eyes (which reflects measurement variability over 5 weeks follow-up) and the Longitudinal Group eyes (which reflects aging and glaucoma progression over two years follow-up) are presented in Table 3. In eyes from the Variability Group, mean rates of MRW, macular GC-IPL thickness change and cpRNFL thickness change were, −0.09 μm/year ($p = 0.69$), and −0.008 μm/year ($p = 0.74$) and −0.01 μm/year ($p = 0.87$), respectively, confirming stability (i.e., all $p > 0.05$).

In advanced glaucoma eyes from the Longitudinal Group, the mean rates of MRW, macular GC-IPL thickness change and cpRNFL thickness change were, −1.51 μm / year ($p = 0.03$), −0.21 μm / year ($p < 0.001$) and −0.36 μm / year ($p = 0.02$), respectively. All changes were statistically significant from baseline to approximately two years of follow-up. Based on the

Variability Group, 1st percentile CIs (i.e., cut-offs used to define change) were −0.32 for MRW, −0.02 for GC-IPL and −1.0 cpRNFL (Table 3). In addition, there was no association between image signal-to-noise ratio (SNR, Mean = 25.33, S.D. ±4.11) and rate of change of MRW (ρ=0.17, p=0.49), GC-IPL (ρ=0.09. p=0.35) or cpRNFL (ρ=0.23, p=0.71).

The mean percentage of image area that did not reach the floor in the baseline images of eyes in the Longitudinal Group (i.e., the image percentage that changed after two years of follow-up) was 19% for MRW, 36% for GC-IPL thickness and 14% for cpRNFL thickness, indicating that GC-IPL likely is the most robust measurement for assessing localized change in eyes with advanced glaucoma. Mean rates of change of MRW, GC-IPL and cpRNFL were not significant in areas reaching the estimated measurement floors in the Longitudinal Group (all p≥0.41), but were significant in areas that did not reach the estimated floor (all p<0.001) (Table 4).

Using the estimated measurement variability from the Variability Group, the measurement floors were 105 μm (±15.9) for MRW, 38 μm (±3.4) for GC-IPL thickness and 38 μm (±4.2) for cpRNFL thickness. These values are specific to our Variability Group only and are not necessarily indicative of measurement floors observed in other or larger groups. These values were used only to provide descriptions of the tissue remaining that was usable for detecting progression (i.e., the diagnostic tissue) in more advanced glaucoma and to compare the possible change in the different tissues in the same advanced glaucoma eyes over time.

Figure 1 shows color-coded examples of whole image GC-IPL thickness (top) and cpRNFL thickness (bottom) measurements from baseline images of an eye in the Longitudinal Group with areas that have reached the defined respective floors shaded.

DISCUSSION

The current study estimated the measurements below which no further change in SD-OCT-measured MRW, GC-IPL thickness and cpRNFL thickness could be observed (i.e., the measurement floors) in glaucoma eyes. These results indicate that changes in SD-OCT measurements are possible in advanced glaucoma (MD ≤ −12 dB), and that such changes are observable over a relatively short period of time, suggesting the usefulness of SD-OCT monitoring for progression detection in this population.

Moreover, we found SD-OCT measured ganglion cell-inner plexiform layer thickness was the least likely parameter to reach the floor across the majority of the image area at baseline, suggesting this parameter is the most informative of the parameters investigated for detecting disease-related change in advanced glaucoma and supporting the long-held idea that the macular region is preserved latest in the glaucoma disease process. One recently published study has suggested the same. Belghith and colleagues[24] showed that in 35 very advanced glaucoma eyes (MD ≤−21 dB) imaged longitudinally for approximately 3.5 years (at approximately 6 months intervals) using Spectralis SD-OCT, significant change in GC-IPL thickness was detected in 31% of eyes compared to 11% and 5% for MRW and cpRNFL thickness, respectively. In addition, in these very advanced eyes, the mean rate of change of

GC-IPL was significantly different from zero whereas this was not the case for MRW and cpRNFL. The mean macular GC-IPL thickness tended to be greater at baseline in the eyes that showed progression than in the eyes that did not, suggesting that progressing eyes had not reached the floor at baseline. It should be noted that glaucoma eyes in the Belghith et al., study were significantly more advanced at baseline than eyes in the current study.

To our knowledge, our results are the first attempt to describe the measurement floors locally across whole SD-OCT images. However, several earlier studies have used a variety of methods to estimate the measurement floor for cpRNFL thickness using various methods with varying results. Sihota et al.[25], utilized cross-sectional analysis of Stratus time-domain OCT (TD-OCT) circle scans to estimate an average RNFL thickness floor of 44.93 μm (±4.95 μm) in 17 eyes blinded by glaucoma (no light perception). In addition, they reported average RNFL thickness of 53.65 μm (±14.20 μm) in 25 eyes with SAP MD ≤ −12 dB (i.e., severe glaucoma by our current definition), suggesting that the potential for detecting disease-related change in advanced glaucoma already existed with an earlier generation instrument with comparatively limited image resolution. Hood and colleagues[7] measured cpRNFL thickness in 15 glaucoma eyes across a range of glaucoma severities (SAP MD −2.7 dB to −16.11 dB) using the Stratus TD-OCT fast circle scan protocol (256 A-scans) and tested the applicability of a previously described linear structure versus function model in which the cpRNFL thickness floor based on the assumption that at visual field MD worse than −10 dB, RNFL thickness reaches an asymptotic floor).[26] Using this assumption, they estimated the RNFL measurement floor at 53.7 μm (±14.2 μm) (see also[27] for similar results). Using the same method with a −10dB cut-off on independent data sets of glaucoma eyes and anterior ischemic optic neuropathy eyes, the cpRNFL thickness measurement floor ranged from 45.5 μm to 50.5 μm[28]).

More recently, Mwanza and colleagues used Bayesian analysis methods to estimate the tipping point at which measurable cpRNFL thinning ends (i.e., the cpRNFL measurement floor).[9] Using cpRNFL thickness measurements obtained from Spectralis and RTVue circle scan protocols. Calculated global cpRNFL floors were 49.9 μm for Spectralis and 70.6 μm for RTVue at SAP MDs of −25.1 dB and −18.9 dB, respectively. Although the estimated Spectralis cpRNFL thickness floor reported by Mwanza et al. was similar to that described by Hood and colleagues, the RTVue-measured thickness floor was not. This difference likely is attributable to different reported RNFL thickness measurements between instruments (e.g., Leite et al.[29]). Dramatic differences in reported SAP MD cut-points between Hood and colleagues and Mwanza and colleagues (visual field MD ≤ −10 dB versus ≤ −18 dB or worse) may be attributable to differences in analysis strategies (use of a simple linear model versus a Bayesian analysis method). In fact, in another study, Mwanza et al. compared their method of estimating the structure versus function tipping point to the simple linear model proposed by Hood et al. and found more similar SAP MD cut-points using the simple linear model in their independent data set (ranging from visual field MD −10.4 dB for Cirrus to −14.4 dB for RTVue) and similar cpRNFL thickness floors, supporting a likely explanation for the differences in results was due to differences in methods used to define thickness floors.

The measurement floor for cpRNFL thickness reported in the current study is not directly comparable to those described above because it was estimated based on variability in stable glaucoma eyes and was not directly observed or related to a proposed SAP MD cut-off. It would not have been appropriate to use the thickness floors reported from other studies as our cut-offs, because we estimated the floor across the entire available image instead of under an instrument defined circle scan.

A criticism of the current study may be that because we estimated the MRW, GC-IPL and cpRNFL thickness floors based on variability in stable glaucoma eyes using an arbitrary variability cut-off, our estimated floor results are not accurate and therefore our percent-image-area-preserved-relative-to-image-floor results reported from baseline measurements in the Longitudinal Group are not accurate. While this might be the case, we argue that no matter the cut-off chosen, the *relative* results among the investigated parameters would remain similar.

We also did not require a minimum Spectralis image quality metric, SNR, cut-off (although SNR was reported). This is because SNR is a global assessment and we assessed local measurements. Image quality likely varies locally over the whole image so we individually assessed each image to assure that the measurement-specific region of interest was well focused and without any image-related artifacts. Recall that the overall quality of each OCT scan was considered good based on our standardized assessment protocol. Because of this, it is possible that our images did not represent images obtained in a typical glaucoma clinic that, in some cases, may not be assessed for quality beyond SNR.

One could argue that any image area defined as a floor measurement in the current study was a stable area that simply did not show change over time. However, these areas were not apparently diagnostic of glaucomatous progression (or progression due to aging) because no statistical change was observed. Reported thicknesses in floor regions were less thick than the glaucoma progression diagnostic areas (i.e., image areas that showed significant change over time, Table 4) suggesting that, for our advanced glaucoma eyes, these areas had in fact reached the measurement floor.

Despite these possible criticisms, we believe that the strengths and innovation of this study are that we are investigating multiple newly available parameters, measured longitudinally on whole images in advanced glaucoma eyes. Most importantly, this study serves as a proof-of-concept that SD-OCT measurements are sensitive to disease-related change in advanced glaucoma, particularly in specific regions of the image. Longer follow-up and investigation of various cut-off definitions to define measurement floors would provide added information, but are beyond the scope of the current study.

In conclusion, the current study showed that a significant percentage of SD-OCT-measured retinal tissue is spared from the measurement floor in advanced glaucoma eyes. In addition, progressive thinning of the spared tissue is observable well into late-stage disease, particularly when GC-IPL thickness is the structural parameter measured. These results indicate that optical imaging, particularly SD-OCT imaging, has a place in detecting structural change in eyes with advanced glaucoma. These finding have strong clinical

implications because treatment decisions rely on determining whether a patient is stable or progressing. These decisions are most important in advanced glaucoma patients, who are at the greatest risk of becoming functionally impaired or blind from the disease and are the most expensive to manage.[30]

Acknowledgments

Funding/Support:

NIH R01EY022039, U10EY014267, P30EY022589, R01EY011008, R01EY019869, R01EY021818 and participant incentive grants in the form of glaucoma medication at no cost from Alcon Laboratories Inc., Allergan Inc., and Pfizer Inc.

REFERENCES

1. Weinreb RN, Aung T, Medeiros FA. The pathophysiology and treatment of glaucoma: a review. JAMA. 2014; 311(18):1901–1911. [PubMed: 24825645]
2. Weinreb RN, Khaw PT. Primary open-angle glaucoma. Lancet. 2004; 363(9422):1711–1720. [PubMed: 15158634]
3. Hood DC, Raza AS, de Moraes CG, Johnson CA, Liebmann JM, Ritch R. The Nature of Macular Damage in Glaucoma as Revealed by Averaging Optical Coherence Tomography Data. Transl Vis Sci Technol. 2012; 1(1):3.
4. Hood DC, Raza AS, de Moraes CG, Liebmann JM, Ritch R. Glaucomatous damage of the macula. Prog Retin Eye Res. 2013; 32:1–21. [PubMed: 22995953]
5. Hood DC, Slobodnick A, Raza AS, de Moraes CG, Teng CC, Ritch R. Early glaucoma involves both deep local, and shallow widespread, retinal nerve fiber damage of the macular region. Invest Ophthalmol Vis Sci. 2014; 55(2):632–649. [PubMed: 24370831]
6. Raza AS, Cho J, de Moraes CG, et al. Retinal ganglion cell layer thickness and local visual field sensitivity in glaucoma. Arch Ophthalmol. 2011; 129(12):1529–1536. [PubMed: 22159673]
7. Hood DC, Anderson SC, Wall M, Kardon RH. Structure versus function in glaucoma: an application of a linear model. Invest Ophthalmol Vis Sci. 2007; 48(8):3662–3668. [PubMed: 17652736]
8. Hood DC, Kardon RH. A framework for comparing structural and functional measures of glaucomatous damage. Prog Retin Eye Res. 2007; 26(6):688–710. [PubMed: 17889587]
9. Mwanza JC, Budenz DL, Warren JL, et al. Retinal nerve fibre layer thickness floor and corresponding functional loss in glaucoma. Br J Ophthalmol. 2015; 99(6):732–737. [PubMed: 25492547]
10. Mwanza JC, Kim HY, Budenz DL, et al. Residual and Dynamic Range of Retinal Nerve Fiber Layer Thickness in Glaucoma: Comparison of Three OCT Platforms. Invest Ophthalmol Vis Sci. 2015; 56(11):6344–6351. [PubMed: 26436887]
11. Banister K, Boachie C, Bourne R, et al. Can Automated Imaging for Optic Disc and Retinal Nerve Fiber Layer Analysis Aid Glaucoma Detection? Ophthalmology. 2016; 123(5):930–938. [PubMed: 27016459]
12. Radius RL, Anderson DR. The histology of retinal nerve fiber layer bundles and bundle defects. Arch Ophthalmol. 1979; 97(5):948–950. [PubMed: 109068]
13. Ye C, Yu M, Leung CK. Impact of segmentation errors and retinal blood vessels on retinal nerve fibre layer measurements using spectral-domain optical coherence tomography. Acta Ophthalmol. 2016; 94(3):e211–e219. [PubMed: 26132774]
14. Artes PH, Iwase A, Ohno Y, Kitazawa Y, Chauhan BC. Properties of perimetric threshold estimates from Full Threshold, SITA Standard, and SITA Fast strategies. Invest Ophthalmol Vis Sci. 2002; 43(8):2654–2659. [PubMed: 12147599]
15. Heijl A, Lindgren A, Lindgren G. Test-retest variability in glaucomatous visual fields. Am J Ophthalmol. 1989; 108(2):130–135. [PubMed: 2757094]

16. Wall M, Woodward KR, Doyle CK, Artes PH. Repeatability of automated perimetry: a comparison between standard automated perimetry with stimulus size III and V, matrix, and motion perimetry. Invest Ophthalmol Vis Sci. 2009; 50(2):974–979. [PubMed: 18952921]
17. Sample PA, Girkin CA, Zangwill LM, et al. The African Descent and Glaucoma Evaluation Study (ADAGES): design and baseline data. Arch Ophthalmol. 2009; 127(9):1136–1145. [PubMed: 19752422]
18. Hodapp, E., Parrish, PK., Anderson, DR. Clinical Decisions in Glaucoma. Mosby: St. Louis; 1993.
19. Belghith A, Bowd C, Medeiros FA, et al. Does the Location of Bruch's Membrane Opening Change Over Time? Longitudinal Analysis Using San Diego Automated Layer Segmentation Algorithm (SALSA). Invest Ophthalmol Vis Sci. 2016; 57(2):675–682. [PubMed: 26906156]
20. Belghith, A., Bowd, C., Medeiros, FA., Weinreb, RN., Zangwill, LM. Automated segmentation of anterior lamina cribrosa surface: How the lamina cribrosa responds to intraocular pressure change in glaucoma eyes; Biomedical Imaging (ISB), 2015 IEEE 12th International Symposium on; 2015. p. 222-225.
21. Belghith, A., Bowd, C., Yang, Z., Medeiros, FA., Weinreb, RN., ZAngwill, LM. Measurement of BMO plane-based anterior lamina cribrosa surface depth (ALCSD) parameters using a deconvolution approach applied to 3D spectral domain optical coherence tomograph optic nerve head images. Association for Research in Vision and Ophthalmology 2014 ISIE/Imaging Conference; 2014; Orlando, FL.
22. Belghith, A., Collet, C. Computational Surgery and Dual Training. New York: Springer; 2014. Armspach. A statistical framework for biomarker analysis and hr-mas 2d metabolite identification; p. 89-112.
23. Rohrschneider K. Determination of the location of the fovea on the fundus. Invest Ophthalmol Vis Sci. 2004; 45(9):3257–3258. [PubMed: 15326148]
24. Belghith A, Medeiros FA, Bowd C, et al. Structural change can be detected in advanced glaucoma eyes. Invest Ophthalmol Vis Sci. In Press.
25. Sihota R, Sony P, Gupta V, Dada T, Singh R. Diagnostic capability of optical coherence tomography in evaluating the degree of glaucomatous retinal nerve fiber damage. Invest Ophthalmol Vis Sci. 2006; 47(5):2006–2010. [PubMed: 16639009]
26. Hood DC. Relating retinal nerve fiber thickness to behavioral sensitivity in patients with glaucoma: application of a linear model. J Opt Soc Am A Opt Image Sci Vis. 2007; 24(5):1426–1430. [PubMed: 17429489]
27. Kim SH, Jeoung JW, Park KH, Kim TW, Kim DM. Correlation between retinal nerve fiber layer thickness and visual field sensitivity: diffuse atrophy imaging study. Ophthalmic Surg Lasers Imaging. 2012; 43(6 Suppl):S75–S82. [PubMed: 23357328]
28. Hood DC, Anderson S, Rouleau J, et al. Retinal nerve fiber structure versus visual field function in patients with ischemic optic neuropathy. A test of a linear model. Ophthalmology. 2008; 115(5): 904–910. [PubMed: 17870170]
29. Leite MT, Rao HL, Weinreb RN, et al. Agreement among spectral-domain optical coherence tomography instruments for assessing retinal nerve fiber layer thickness. Am J Ophthalmol. 2011; 151(1):85 e81–92 e81. [PubMed: 20970108]
30. Traverso CE, Walt JG, Kelly SP, et al. Direct costs of glaucoma and severity of the disease: a multinational long term study of resource utilisation in Europe. Br J Ophthalmol. 2005; 89(10): 1245–1249. [PubMed: 16170109]

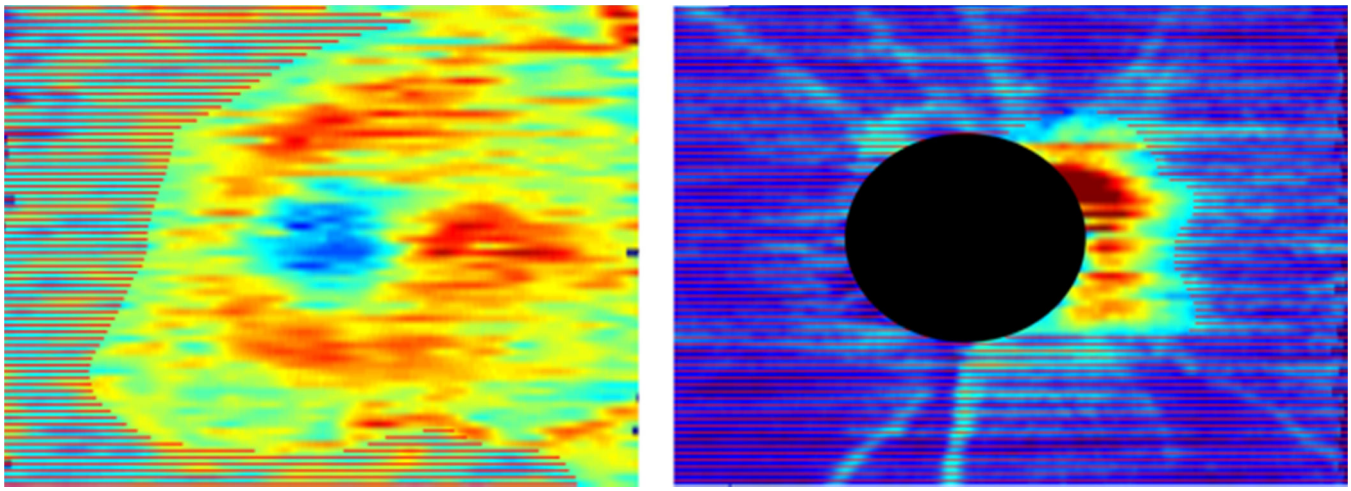

Figure 1.

Color-coded examples of whole image ganglion cell-inner plexiform layer thickness (left) and circumpapillary retinal nerve fiber layer thickness (right) measurements from baseline images of an advanced glaucoma eye in the Longitudinal Group with areas that have reached the defined respective floors shaded (SAP MD = −17.9 dB in this eye).

Table 1

Demographic, ocular and visual field measurements in eyes composing the Variability Group and Longitudinal Group at baseline SD-OCT imaging date.

	Variability Group	Longitudinal Group	P=
Number of eyes	41	87	
Sex, % female	61	59	0.68
Age in years (SD)	70.0 (±7.9)	73.0 (±9.4)	<0.001
Number of visits	5	2	<0.001
Follow-up time (SD)	5 weeks	1.8 (±0.3) years	<0.001
Axial length in mm (SD)	24.1 (±1.9)	23.95 (±1.4)	0.44
Disc area in mm^2 (SD)	2.17 (±0.5)	2.10 (±0.4)	0.41
Visual field Mean deviation in dB (range)	−10.4 (−8.3, −23.0)	−17.0 (−12.5, −27.0)	<0.001

Table 2

Baseline mean global minimum rim width, macular ganglion cell-inner plexiform layer thickness and circumpapillary retinal nerve fiber layer thickness measurements by study group.

	Variability Group	Longitudinal Group	P=
MRW in μm (SD)	155.1 (±16.4)	141.8 (±15.3)	<0.001
GC-IPL in μm (SD)	71.3 (±9.3)	62.8 (±10.4)	<0.001
cpRNFL μm (SD)	67.4 (±7.9)	61.4 (±6.7)	<0.001

MRW = minimum rim width
GC-IPL = Ganglion Cell-Inner Plexiform Layer
cpRNFL = Circumpapillary Retinal Nerve Fiber Layer

T-test p-values reported represent the differences between stable variability eyes and longitudinal eyes.

Table 3

Annual rates of global minimum rim width, macular ganglion cell-inner plexiform layer thickness and circumpapillary retinal nerve fiber layer thickness loss by study group.

	Variability Group			Longitudinal Group			*P=
	Mean	99th Percentile CI	P=	Mean	95% CI	P=	
MRW (μm/year)	−0.09	(−0.32, 0.44)	0.69	−1.51	(−2.30, 0.40)	<0.03	<0.001
GC-IPL (μm/year)	−0.008	(−0.02, 0.02)	0.74	−0.21	(−0.29, 0.04)	<0.01	<0.001
cpRNFL(μm/year)	−0.01	(−0.10, 0.15)	0.87	−0.36	(−0.62, 0.07)	<0.02	<0.001

MRW = minimum rim width
GC-IPL = Ganglion Cell-Inner Plexiform Layer
cpRNFL = Circumpapillary Retinal Nerve Fiber Layer

*P evaluates differences in the mean rate of change between stable and longitudinal groups.

Table 4

Baseline tissue thickness and annual rates of global minimum rim width, macular ganglion cell-inner plexiform layer thickness and circumpapillary retinal nerve fiber layer thickness loss by glaucoma progression detection areas in the advanced glaucoma Longitudinal Group.

	Floor Areas			Diagnostic Areas			P=*
Baseline Thickness	**Mean**	**95th CI**		**Mean**	**95%CI**		
MRW (μm)	105.57	(76.35,144.40)		187.59	(161.23, 213.48)		<0.001
GC-IPL (μm)	38.01	(32.61, 42.75)		79.52	(61.32, 91.03)		<0.001
cpRNFL (μm)	38.20	(31.15, 44.89)		81.13	(68.11, 99.51)		<0.001
Slope	**Mean**	**95th CI**	**P=**	**Mean**	**95%CI**	**P=**	<0.001
MRW (μm/year)	−0.060	(−0.68, 0.51)	0.41	−2.71	(−3.04, −0.23)	<0.001	<0.001
GC-IPL (μm/year)	−0.015	(−0.05, 0.031)	0.65	−0.33	(−0.46, −0.07)	<0.001	<0.001
cpRNFL(μm/year)	−0.023	(−0.19, 0.12)	0.74	−0.52	(−0.89, −0.14)	<0.001	<0.001

MRW = minimum rim width
GC-IPL = Ganglion Cell-Inner Plexiform Layer
cpRNFL = Circumpapillary Retinal Nerve Fiber Layer

*P evaluates differences in the mean baseline tissue thickness or rate of change between floor areas and diagnostic areas.